Communication

Room-Temperature Wurtzite ZnS Nanocrystal Growth on Zn Finger-like Peptide Nanotubes by Controlling Their Unfolding Peptide Structures

Ipsita A. Banerjee, Lingtao Yu, and Hiroshi Matsui

J. Am. Chem. Soc., **2005**, 127 (46), 16002-16003• DOI: 10.1021/ja054907e • Publication Date (Web): 28 October 2005

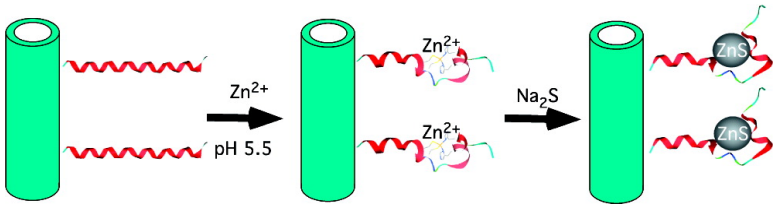

More About This Article

Additional resources and features associated with this article are available within the HTML version:

- Supporting Information
- Links to the 12 articles that cite this article, as of the time of this article download
- Access to high resolution figures
- Links to articles and content related to this article
- Copyright permission to reproduce figures and/or text from this article

View the Full Text HTML

J|A|C|S
COMMUNICATIONS

Published on Web 10/28/2005

Room-Temperature Wurtzite ZnS Nanocrystal Growth on Zn Finger-like Peptide Nanotubes by Controlling Their Unfolding Peptide Structures

Ipsita A. Banerjee, Lingtao Yu, and Hiroshi Matsui*

Department of Chemistry and Biochemistry at Hunter College and the Graduate Center, The City University of New York, New York, New York 10021

Received July 21, 2005; E-mail: hmatsui@hunter.cuny.edu

A class of wide-gap II−VI semiconductor nanomaterials has shown interesting optical, electrical, and optoelectric properties via quantum confinement.[1,2] ZnS nanocrystals have attracted considerable attention due to its applications in flat-panel displays, electroluminescent devices, infrared windows, sensors, and lasers.[3] For those applications, phase controls of ZnS nanocrystals were critical to tune their physical properties to the appropriate ones. From the industrial point of view, the wurtzite ZnS nanocrystal fabrication at room temperature is extremely practical; however, the most stable ZnS structure in nanoscale is the zinc blende (cubic) structure,[4] and scientists have just begun exploring the room-temperature synthesis of the wurtzite structure of ZnS nanocrystals. One promising approach for the room-temperature nanocrystal synthesis is to use biological templates because biomineralization in nature crystallizes many types of nanoparticles at room temperature by using proteins and peptides.[5] For example, peptide sequences were identified by phage display libraries to grow the wurtzite ZnS nanocrystals and the zinc blende ZnS nanocrystals, respectively.[2] Histidine, which binds Zn ions in Zn finger peptides, was also used to grow wurtzite ZnS nanocrystals at room temperature.[6] While those approaches could mimic biological systems to grow the targeted nanocrystal structure at room temperature, how peptides control nucleations and crystalline phases is not clear enough to apply them to synthesize specific nanocrystal structures in general.

Recently, in the high-temperature synthesis of ZnS nanobelts, sizes of seed crystals could control their final crystalline structures.[3] For example, Au catalyst particles smaller than 50 nm nucleated the zinc blende structure, while particles larger than 100 nm nucleated the wurtzite structure via vapor deposition technique. In this communication, we combined the peptide template approach and the nucleation-site controlling approach to control the phase of ZnS nanocrystals to the wurtzite structure at room temperature. Peptide nanotubes, consisting of the M1 peptide (VAL-CYS-ALA-THR-CYS-GLU-GLN-ILE-ALA-ASP-SER-GLN-HIS-ARG-SER-HIS-ARG-GLN-MET-VAL) that is synthesized based on the peptide motif of the Influenza Virus Matrix Protein M1, could grow the wurtzite ZnS nanocrystals on the nanotube templates in solution. The M1 protein controls ribonucleoprotein (RNP) coatings on the virus as a function of pH, which plays a crucial role in the virus replication.[7] In the M1 protein, the unfolding process of the helical M1 peptide backbone motif via pH change creates a linker region between N- and C-terminated helical domains that contains a Zn finger-like Cys_2His_2 motif.[8] Because the higher pH increases the uptake of Zn ions in the Cys_2His_2 motif of the M1 peptide by unfolding more helical domains, the pH change can essentially control the size and the number of the nucleation sites in the M1 peptides to grow ZnS nanocrystals with desired phases. Here we optimized the nucleation sites in the M1 peptides by unfolding them with pH to obtain monodisperse and crystalline wurtzite ZnS nanocrystals on the template nanotubes at room temperature (Figure 1).

Previously, the template nanotubes, self-assembled from peptide bolaamphiphile monomers via three-dimensional hydrogen bonds between amide and carboxylic acid groups, were coated by various synthetic peptides on the nanotube surfaces to grow metal nanoparticles on the templates.[9] These peptides were bound to free amide groups of the nanotubes via hydrogen bonding with a simple incubation process. To immobilize the M1 peptides on the template nanotubes, 50 μL of the M1 peptide in a pH 7 buffer was incubated with 100 μL of the nanotube solution (10 mM) for 24 h. For the ZnS nanocrystal growth on the M1 peptide nanotubes, 20 μL of zinc 2,9,16,23-tetrakis(phenylthio)-29*H*,31*H*-phtanlocyanine solution (50 μM in 70% THF) was added to the peptide nanotube solution to bind Zn(II) ions to the linker regions of the M1 peptides that contain the Zn finger-like Cys_2His_2 motifs (Figure 1b). After pHs of the growth solutions were adjusted between 5.0 and 10.0, 0.1 mL of 0.5 M Na_2S solution was added at 10 °C and sat for 24 h under N_2 to grow ZnS nanocrystals on the nanotubes (Figure 1c). The detailed experimental procedure is in Supporting Information. Figure 2a shows a transmission electron micrograph (TEM) of ZnS nanocrystals grown on the nanotubes at pH 5.5. Those nanocrystals were monodisperse with an average diameter of 4 nm when they were grown in pH 5.5−7.4. When the same coating procedure was applied to the template nanotubes without the M1 peptide, the coverage of ZnS nanocrystals on the nanotube was significantly diminished, and the polydisperse nanocrystals were aggregated on the nanotube surfaces, as shown in Figure 2b. This comparison indicates that the M1 peptide plays a significant role in regulating the size and the surface coverage of ZnS nanocrystals. When the ZnS nanocrystals were grown on the M1 peptide nanotubes in pH 5.5, the electron diffraction pattern of resulting ZnS nanocrystals shows (002), (110), and (112) phases of the wurtzite structure, as shown in Figure 2c. In the higher pH conditions (pH > 8), the crystalline ZnS could not be obtained on the nanotubes. When ZnS nanoparticles were grown with the M1 peptides without the template nanotubes in the pH range of 5.5−7.4, large aggregates of ZnS particles and the M1 peptides were observed.

The UV/vis spectrum and the fluorescence spectrum (excited at 288 nm) of ZnS nanocrystals on the M1 peptide nanotubes (pH 5.5) show absorption λ_{max} at 280 nm (blue line in Figure 3a) and a fluorescence peak at 439 nm (Figure 3b), respectively. Since no absorption from the M1 peptide nanotubes around 280 nm was observed (red line in Figure 3a), the 280 nm absorption of the blue line in Figure 3a is attributed to ZnS nanocrystals. A small shoulder at 470 nm in Figure 3b corresponds to the defect-related emission of ZnS nanocrystals.[10] These absorption and fluorescence peaks indicate that the band gap of these ZnS nanocrystals in the diameter

10.1021/ja054907e CCC: $30.25

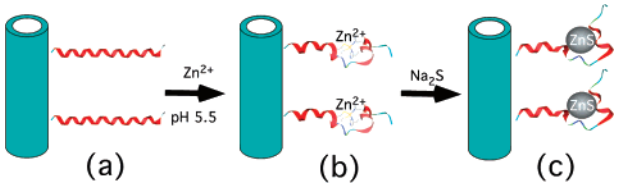

Figure 1. Illustration of the ZnS nanocrystal growth on the unfolding M1 peptides on the template nanotubes as a function of pH.

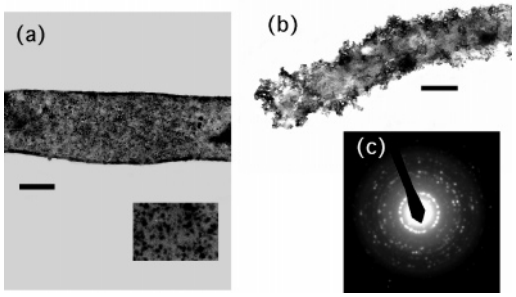

Figure 2. (a) TEM image of ZnS nanocrystals on the M1 peptide nanotubes grown at pH 5.5. Inset: In the high magnification; scale bar = 70 nm. (b) TEM image of ZnS nanocrystals on the neat template nanotubes with no M1 peptides grown at pH 5.5; scale bar = 100 nm. (c) Electron diffraction of the ZnS nanocrystals on the M1 peptide nanotubes grown at pH 5.5.

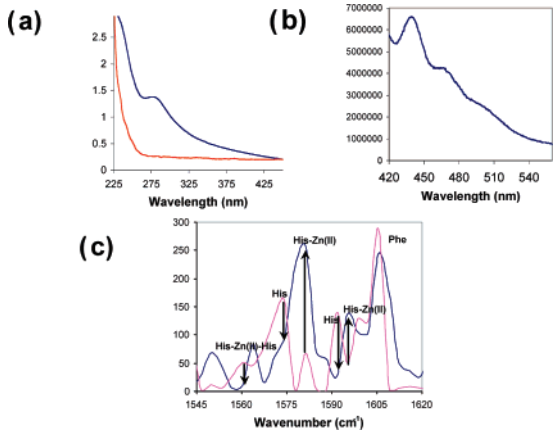

Figure 3. (a) UV/vis spectra of the Zn(II)-bound M1 peptide nanotubes (blue line) and the M1 peptide nanotubes with no Zn(II) (red line). (b) Fluorescence spectrum of the ZnS nanocrystals on the M1 peptide nanotubes. (c) Raman spectra of the Zn(II)-bound M1 peptide nanotubes at pH 5.5 (pink) and at pH 10.0 (blue).

of 4 nm is 4.4 eV, and the peak positions in both UV/vis and fluorescence spectra are consistent with the ones for ZnS nanocrystals, whose diameter is about 4 nm.[1,4,6] The folding M1 peptide conformation and the binding conformations between Zn ions and the M1 peptides were probed by circular dichroism (CD) spectroscopy and Raman microscopy. The change in CD spectra of the M1 peptides on the nanotubes in the presence of Zn ions as a function of pH indicates that the M1 peptide undergoes more unfolding in higher pHs (Supporting Information). When Zn ions were mixed with the M1 peptides at pH 5.5 (red line in Figure 3c), the N(His)−Zn^{2+}−N(His) bond formation was observed at 1561 cm^{-1}.[11] However, as Zn ions were incubated in the pH 10.0 nanotube solution (blue line in Figure 3c), this His−Zn^{2+}−His peak intensity was much weaker, and instead, the peak intensities for the N(His)−Zn^{2+} bond at 1581 and 1595 cm^{-1} were increased.[8,12] This spectral comparison indicates that the unfolding of the M1 peptide on the nanotubes via pH increase induces the extension of the linker region in the helical backbone, which favors the His−Zn^{2+} chelation over the His−Zn^{2+}−His chelation. The decrease of the imidazole peak of the neat histidine via pH increase shows that more Zn ions were taken up by histidines of the M1 peptide at higher pHs, which is consistent with previous observation.[8] The crystallinity difference of ZnS nanocrystals between acidic and basic conditions may be explained by two chelation structures between Zn ions and histidines. When sulfide ions substitute nitrogens of the Zn(II)−N(His) bonds to grow ZnS in the nucleation stage, the exchange kinetics and the directionality of resulting Zn−S bonds should differ between these two chelating structures. This difference in the nucleation process can influence the crystallinity and the final crystalline structure of nanocrystals. In the case of the M1 peptide nanotube, the Zn(II)−Cys_2His_2 motif was the right nucleation structure to grow the wurtzite ZnS nanocrystals at room temperature.

In conclusion, monodisperse ZnS nanocrystals were grown on the M1 peptide-coated nanotubes at room temperature. When pH of the growth solution was adjusted to 5.5, ZnS nanocrystal was grown as the highly crystalline wurtzite, and the structure became more amorphous as pH was raised to 10.0, controlled by the unfolding conformation of the M1 peptides. This concept should be widely applicable to other crystal growths to control their structures by optimizing peptide sequences and conformations.

Acknowledgment. This work was supported by the U.S. Department of Energy (DE-FG-02-01ER45935). I.B. thanks Dr. A. Tsiola at the Core Facilities for Imaging at Queens College−CUNY for TEM. L.Y. thanks Prof. Y. Xu at Hunter College for CD spectroscopy.

Supporting Information Available: Experimental procedures for the M1 peptide coating on template nanotube and the wurtzite ZnS nanocrystal growth, instrumentations, CD spectra of the M1 peptides, and additional TEM images of ZnS-coated nanotubes. This material is available free of charge via the Internet at http://pubs.acs.org.

References

(1) Zhang, H. Z.; Gilbert, B.; Huang, F.; Banfield, J. F. *Nature* **2003**, *424*, 1025.

(2) Flynn, C. E.; Mao, C. B.; Hayhurst, A.; Williams, J. L.; Georgiou, G.; Iverson, B.; Belcher, A. M. *J. Mater. Chem.* **2004**, *13*, 2414.

(3) Ding, Y.; Wang, X. D.; Wang, Z. L. *Chem. Phys. Lett.* **2004**, *398*, 32.

(4) Zhao, Y. W.; Zhang, Y.; Zhu, H.; Hadjipianayis, G. C.; Xiao, J. Q. *J. Am. Chem. Soc.* **2004**, *126*, 6874.

(5) (a) Naik, R. R.; Stringer, S. J.; Agarwal, G.; Jones, S. E.; Stone, M. O. *Nat Mater.* **2002**, *1*, 169. (b) Cha, N. J.; Stucky, G. D.; Morse, D. E.; Deming, T. J. *Nature* **2000**, *403*, 289. (c) Sarikaya, M.; Tamerler, C.; Jen, A. K. Y.; Schulten, K. *Nat. Mater.* **2003**, *2*, 577. (d) Slocik, J. M.; Moore, J. T.; Wright, D. W. *Nano Lett.* **2002**, *2*, 169. (e) Reches, M.; Gazit, E. *Science* **2003**, *300*, 625. (f) Bansal, V.; Sanyal, A.; Rautaray, D.; Ahmad, A.; Sastry, M. *Adv. Mater.* **2005**, *17*, 889. (g) Douglas, T.; Strable, E.; Willits, D.; Aitouchen, A.; Libera, M.; Young, M. *Adv. Mater.* **2002**, *14*, 415. (h) Sano, K. I.; Sasaki, H.; Shiba, K. *Langmuir* **2005**, *21*, 3090. (i) Park, S. H.; Barish, R.; Li, H. Y.; Reif, J. H.; Finkelstein, G.; Yan, H.; LaBean, T. H. *Nano Lett.* **2005**, *5*, 693.

(6) Kho, R.; Nguyen, L.; Torres-Martinez, C. L.; Mehra, R. K. *Biochem. Bioph. Res. Commun.* **2000**, *272*, 29.

(7) Zoueva, O. P.; Bailly, J. E.; Nicholls, R.; Brown, E. G. *Virus Res.* **2002**, *85*, 141.

(8) Okada, A.; Miura, T.; Takeuchi, H. *Biochemistry* **2003**, *42*, 1978.

(9) (a) Banerjee, I. A.; Yu, L.; Matsui, H. *Proc. Natl. Acad. Sci. U.S.A.* **2003**, *100*, 14678. (b) Yu, L.; Banerjee, I. A.; Matsui, H. *J. Am. Chem. Soc.* **2003**, *125*, 14837. (c) Yu, L.; Banerjee, I. A.; Shima, M.; Rajan, K.; Matsui, H. *Adv. Mater.* **2004**, *16*, 709. (d) Djalali, R.; Chen, Y.-f.; Matsui, H. *J. Am. Chem. Soc.* **2003**, *125*, 5873.

(10) (a) Zhu, Y.-C.; Bando, Y.; Xue, D.-F. *Appl. Phys. Lett.* **2003**, *82*, 1769. (b) Chakraborty, I., Moulik, S. P. *J. Dispersion Sci. Technol.* **2004**, *25*, 849.

(11) Miura, T.; Suzuki, K.; Kohata, N.; Takeuchi, H. *Biochemistry* **2000**, *39*, 7024.

(12) Miura, T.; Satoh, T.; Takeuchi, H. *Biochim. Biophys. Acta* **1998**, *1384*, 171.

JA054907E